

26 **Abstract**

27 Oil is frequently used as a solvent to inject lipophilic substances into the peritoneum of
28 laboratory animals. Although mineral oil causes chronic peritoneal inflammation, little is known
29 whether other oils are better suited. Here we show that olive, peanut, corn or mineral oil causes
30 xanthogranulomatous inflammation with depletion of resident peritoneal macrophages.
31 However, there were striking differences in the severity of the inflammatory response. Peanut
32 and mineral oil caused severe chronic inflammation with persistent neutrophil and monocyte
33 recruitment, expansion of the vasculature and fibrosis. Corn and olive oil provoked no or only
34 mild signs of chronic inflammation. Mechanistically, the vegetal oils were taken up by
35 macrophages leading to foam cell formation and induction of cell death. Olive oil triggered
36 caspase-3 cleavage and apoptosis, which facilitates the resolution of inflammation. Peanut oil
37 and, to a lesser degree, corn oil triggered caspase-1 activation and macrophage pyroptosis,
38 which impairs the resolution of inflammation. As such, intraperitoneal oil administration can
39 interfere with the outcome of subsequent experiments. As a proof-of-principle, intraperitoneal
40 peanut oil injection was compared to its oral delivery in a thioglycolate-induced peritonitis
41 model. The chronic peritoneal inflammation due to peanut oil injection impeded the proper
42 recruitment of macrophages and the resolution of inflammation in this peritonitis model. In
43 summary, the data indicate that it is advisable to deliver lipophilic substances like tamoxifen
44 by oral gavage instead of intraperitoneal injection.

45

46 **Introduction**

47 Oil is frequently used as solvent in animal research. For instance, inducible gene
48 recombination using the Cre-ERT2 -loxP system requires administration of tamoxifen which is
49 usually dissolved in olive, peanut, corn or mineral oil. The oil solution is administered orally or
50 by intraperitoneal injection (*i.p.*) (1, 2). Also, in a liver fibrosis model carbon tetrachloride (CCl₄)
51 is delivered by *i.p.* injection in oil, inhalation or oral gavage (3). Interestingly, *i.p.* injection
52 generates stronger liver fibrosis when compared with the other two administration methods (4),

53 raising the question whether CCl₄ or its solvent act locally within the peritoneum. Indeed, *i.p.*
54 injection of mineral oil causes chronic inflammation (5-9). Also, subcutaneous injection of olive
55 oil can cause lipogranuloma, a granulomatous inflammatory soft tissue reaction (10).

56 Therefore, it can be assumed that any experimental immune cell analysis within the
57 peritoneal cavity would be strongly affected by oil. It is surprising how little is known about the
58 peritoneal immune cell reaction towards oil and comparative studies of different oils are
59 missing to our knowledge.

60 Peritoneal inflammation can be divided into the initiation and resolution phase.
61 Pathogens trigger infiltration of neutrophils, which phagocytose pathogens, clear apoptotic
62 cells and recruit monocytes from the blood stream into the peritoneal fluid. Recruited
63 monocytes eliminate dying neutrophils and differentiate into monocyte-derived macrophages
64 (11). This is important, as the number of resident peritoneal macrophages, which are derived
65 from embryonic progenitors and have self-renewal capacity (12), get strongly decreased as a
66 result of the so-called “macrophage disappearance reaction” (13). As such, resident peritoneal
67 CD11b⁺ macrophages, expressing high F4/80 levels (F4/80^{hi}) get replaced by monocyte-
68 derived CD11b⁺ macrophages, expressing low F4/80 levels (F4/80^{low}) on the membrane (12,
69 14, 15). Subsequently, monocyte-derived macrophages increase surface expression of F4/80
70 from a low to an intermediate level (F4/80^{int}) to initiate the resolution phase (16).

71 The switch from inflammatory to resolving macrophages is triggered by phagocytosis
72 of apoptotic cells. Deficiency in this phagocytic process leads to chronic inflammation (17). For
73 instance in atherosclerotic plaques, macrophages take up excessive amounts of lipids and
74 become foam cells, which cannot initiate the resolution phase, perpetuating further neutrophil
75 and monocytes infiltration (18).

76 The aim of this study was to analyze how the most commonly used oils in animal
77 research affect the myeloid cells within the peritoneum and whether this would diminish their
78 capability to resolve the peritoneal inflammation.

79

80 **Materials and methods**

81 **Animal models**

82 The study was approved by institutional and regional animal research committees. All animal
83 procedures were in accordance with institutional guidelines and performed according to the
84 guidelines of the local institution and the local government. Female C57BL/6 mice were group-
85 housed under specific pathogen-free barrier conditions.

86 Administration of peanut (P2144, Sigma-Aldrich, St. Louis, USA), corn (C8267, Sigma- Aldrich,
87 St. Louis, USA), olive (88631, Carl Roth, Germany), mineral oil (HP50.2, Carl Roth, Germany)
88 or 0,9% sterile NaCl (Braun, Germany) in 8 to 12-week-old randomized mice was performed
89 by daily *i.p.* injection of 100 µl for 5 consecutive days or by oral gavage of peanut oil once with
90 100 µl. After three weeks mice were euthanized. For peritoneal lavage, 5 ml of cold PBS
91 (Gibco/Thermo Fisher Scientific, NY, USA) was injected *i.p.* after a careful massage to mobilize
92 cells, peritoneal fluid was collected. Cells were isolated by centrifugation (5 min, 200 g) and
93 suspended in 1 ml of PBS.

94 8 to 12-week-old randomized mice were euthanized and administrated with peanut, olive, corn
95 and mineral oil. After 5 minutes the peritoneal lavage was collected.

96 Three weeks after oil treatment, mice were *i.p.* injected with thioglycolate (2 mg in 1 ml H₂O;
97 B2551, Sigma Aldrich, St. Louis, USA). After 24 or 72 hours mice were sacrificed and
98 peritoneal lavage collected. All groups were randomized.

99

100 **Immunofluorescence and tissue histology**

101 Histological analysis was performed on formalin-fixed paraffin-embedded sections (3 µm).
102 Sections were deparaffinized and rehydrated. For hematoxylin-eosin (H&E) and Sirius Red
103 (Dianova, Germany) staining, sections were processed according to standard protocols. For
104 myeloid cell staining, antigen retrieval at pH 6 with citrate buffer and the primary antibody rabbit
105 anti-mouse CD11b (1:200) (ab133357, Abcam, Cambridge, MA, USA) and antigen retrieval

Alsina-Sanchis et al., Oil depletes resident peritoneal macrophages

106 with 1:20 proteinase K/TE buffer and rat anti-mouse F4/80 (1:100) (T-2006, Dianova,
107 Germany) incubated at 4°C overnight. After washing, sections were incubated with secondary
108 antibodies coupled with HRP (1:200) (DAKO, Agilent Technologies, Santa Clara, CA, USA) for
109 one hour at room temperature. For immunofluorescence staining, antigen retrieval at pH 9 was
110 performed using citrate buffer and sections were incubated with the primary antibody rabbit
111 anti-mouse CD31 (1:50) (ab28364, Abcam, Cambridge, MA, USA) at 4°C overnight. After
112 washing, sections were incubated with secondary antibody (1:200) goat anti-rabbit Alexa
113 Fluor-647 (A21245, Life Technologies/Thermo Fisher Scientific, NY, USA) for 1 hour at room
114 temperature. H&E images were obtained with slide scanner (Zeiss Axio Sacn.Z1, Carl Zeiss,
115 Germany). CD11b images were obtained with widefield microscope (Zeiss Axioplan, Carl
116 Zeiss, Germany). All images were processed with ZENblue software (Carl Zeiss, Germany).
117 Immunofluorescence was imaged at the confocal (LSM 700, Carl Zeiss, Germany) microscope
118 with ZENblack software (Carl Zeiss, Germany). Sections of seven Z-stacks per omentum and
119 mesentery and three random fluorescence images per slide were taken. Numbers of CD31
120 positive vessels per view field and lipid droplet size from H&E images were counted with
121 ImageJ software (NIH, Bethesda, MD, USA).

122

123 **Oil Red O staining**

124 Peritoneal lavage was plated into one well of a 6-well plate on top of coverslips and incubated
125 for 30 min with Dulbecco's modified Eagle's medium (DMEM) (Gibco/ Thermo Fisher Scientific,
126 NY, USA). Afterwards non-adherent cells were removed by careful washing three times with
127 PBS. J774A.1 cells cultured in DMEM with 10% fetal calf serum (Biochrom, UK) were seeded
128 into 12-well plates on coverslips and treated with 100 µl oil in 1 ml medium for four hours. Cells
129 on coverslips were stained with Oil Red O (O0625, Sigma-Aldrich) following the protocol
130 published elsewhere (19) and counterstained with hematoxylin. Images were obtained with
131 widefield microscope (Zeiss Axioplan Carl Zeiss, Germany).

132

133 **Flow cytometry**

134 Cells obtained from peritoneal lavage were washed and erythrocytes lysed with ACK lysis
135 buffer (Gibco/Thermo Fisher Scientific, NY, USA). Cells were suspended at approximately 10^6
136 cells/ml in PBS with 2% FCS. Cell suspensions were incubated with the different fluorophore-
137 coupled primary antibodies for 20 minutes on ice. These antibodies were used: CD45
138 (552848), CD11b (552850), CD19 (560375), Ly6G (560600), Ly6C (560594) and F4/80-like
139 (564227) all from BD Biosciences (Bedford, MA, USA), CD3 (100203) and F4/80 (123128)
140 from BioLegend (St. Diego, CA, USA) and Tim4 (12-5866-82, Life Technologies/Thermo
141 Fisher Scientific, NY, USA). Concentration of the different antibodies was determined by
142 titration. Flow cytometer results in percentage were extrapolated to the total amount of cells
143 obtained from the previous cell counting.

144

145 **Western Blot analysis**

146 Cell lysates were separated by SDS-PAGE and proteins blotted on nitrocellulose membranes.
147 Membranes were blocked with 5% skim milk in TBS with 1% Tween-20. The following primary
148 antibodies were used: CD36 (ab124515), VCP (ab11433) from Abcam (Cambridge, MA, USA),
149 ABCG1 (NB400-132SS, Novus Biologicals, CO, USA), Cleaved-Caspase 3 (Asp175; 9664S),
150 Arginase-1 (D4E3M™; 93668S) from Cell Signaling (Danvers, MA, USA) and Caspase 1
151 (14F468; sc-56036, Santa Cruz Technologies, Dallas, TX, USA). Primary antibodies were
152 incubated overnight at 4°C and appropriate HRP-conjugated secondary antibodies (DAKO,
153 Agilent Technologies, Santa Clara, CA, USA) for 1 hour at room temperature.
154 Chemiluminescence was detected by Pierce ECL Western Blotting Substrate (Thermo Fisher
155 Scientific, NY, USA) and ChemiDoc imaging system (Biorad, Hercules, CA, USA) and
156 quantified with Image Lab 3.0 software (Biorad, Hercules, CA, USA).

157

158 **Quantitative PCR**

Alsina-Sanchis et al., Oil depletes resident peritoneal macrophages

159 RNA was isolated using the innuPREP RNA Mini kit (Analytik Jena, Germany). cDNA was
160 synthesized with the High-Capacity cDNA Reverse Transcription Kit (Applied Biosystems). The
161 cDNA was applied to qPCR using the POWER SYBR Green Master Mix (Applied Biosystems).
162 Fold changes were assessed by $2^{-\Delta\Delta Ct}$ method and normalized with the *CPH* gene. The
163 following primers were used for qPCR: CD36 forward GCAAAACGACTGCAGGTCAA and
164 reverse GGCCATCTCTACCATGCCAA, ABCG1 forward CTTTCCTACTCTGTACCCGAGG
165 and reverse CGGGGCATTCCATTGATAAGG, IL10 forward GCATGGCCCAGAAATCAAGG
166 and reverse GAGAAATCGATGACAGCGCC and CPH forward ATGGTCAACCCACCGTG
167 and reverse TTCTTGCTGTCTTTGGAACCTTTGTC.

168

169 **Cell death detection**

170 J774A.1 cells were plated at 5×10^5 cells per well into a 12 well-plate with 100 μ l of the different
171 oils in 1 ml medium and incubated for four hours. Afterwards, supernatant and attached cells
172 were collected and stained with Annexin V-FITC (640905, BioLegend, St. Diego, CA, USA)
173 and PI (Cayman Chemical, USA) and incubated for 15 minutes on ice. After washing, cells
174 were immediately analyzed by flow cytometry.

175 An apoptosis/necrosis immunofluorescence assay kit (ab176749, Abcam, Cambridge, MA,
176 USA,) was used for detection of necrosis or apoptosis cell death. J774A.1 cells were plated at
177 5×10^5 cells/well into a 24 well-plate on top of a coverslip. To each well, 50 μ l of oil was added
178 in a final volume of 1 ml medium and incubated for two hours. Afterwards, the staining was
179 performed following the manufacturer's protocol. Three fluorescence images of each channel
180 at fixed positions of each triplicate were collected at the wide-field Cell Observer microscope
181 (Carl Zeiss, Germany) with ZENblue software (Carl Zeiss, Germany). FIJI software was
182 employed for the quantification of positive cells of each channel per field.

183 For determination of lactate dehydrogenase activity in the cell supernatant, J774A.1 cells were
184 plated at 5×10^4 cells/well into a 96 well-plate with 100 μ l of medium containing 10 μ l oil in
185 triplicates and incubated for 2 hours. Oleic acid (O1008, Sigma- Aldrich, St. Louis, USA),

Alsina-Sanchis et al., Oil depletes resident peritoneal macrophages

186 diluted in absolute ETOH was added to the medium or mixed with 5 μ l peanut oil when
187 indicated. Then, levels of LDH were detected using the LDH-Cytotoxicity Assay Kit (Ab65393,
188 Abcam, Cambridge, MA, USA) following the manufacturer's protocol.

189

190 **Statistical analysis**

191 GraphPad Prism 8 (GraphPad Software, San Diego, CA, USA) was used to generate graphs
192 and for statistical analysis. Statistical significance was calculated using one-way or two-way
193 ANOVA as indicated in the figure legends. Data sets are presented as mean \pm SD. $P < 0.05$
194 was considered as significant.

195

196

197 **Results**

198 **Macroscopic changes upon intraperitoneal oil injection**

199 Peanut, olive, corn and mineral oil were injected into the peritoneum (*i.p.*) of adult mice
200 for five consecutive days. This mimics a typical protocol for delivering tamoxifen to induce gene
201 recombination in transgenic mice expressing Cre^{ERT2} recombinase (2). Analysis was done
202 three weeks later. As controls, untreated mice and mice treated with peanut oil by oral gavage
203 were used (**Figure 1A**).

204 In contrast to untreated mice or those receiving oil by oral gavage, the *i.p.* injected mice
205 showed macroscopically visible alterations in the peritoneal cavity. Peanut oil was still visible
206 as oil droplets (**Figure 1B**), whereas this was not the case for the other oils. White nodules, in
207 the size of <3 mm, were visible on the surface of liver, diaphragm or colon in mice receiving
208 peanut, olive and mineral oil *i.p.* but not corn oil. The nodules formed due to olive oil treatment
209 were only loosely attached to the organ surfaces, whereas the nodules in mice that were *i.p.*
210 injected with peanut or mineral oil were firmly attached to the liver surface (**Figure 1B**).

211

212 **Xanthogranulomatous inflammation in the peritoneum upon oil injection**

213 Histological analysis revealed no pathological changes in liver (**Figure 1C**) and spleen
214 (**Supplementary Figure 1A**) of mice that received *i.p.* injection of oil. The nodules that were
215 firmly attached to the liver surface in mice treated with peanut or mineral oil could be classified
216 as xanthogranulomas with foamy macrophages and mixed inflammatory background (**Figure**
217 **1C**).

218 Next, we examined the greater omentum. The greater omentum is an organ that filters
219 excessive fluid from the abdominal cavity, senses microorganisms or damaged cells, initiates
220 immune responses and supports repair of damaged organs (20). Omenta of mice treated with
221 oral gavage were indistinguishable from those of untreated mice. However, omenta of mice
222 that received *i.p.* oil injections showed a remarkable change in morphology. The omenta were
223 swollen, darker and had enlarged blood vessels, particularly in mice treated with peanut and
224 mineral oil (**Figure 2A**). Histological analysis revealed that lipid droplet size in adipocytes was
225 reduced in mice treated *i.p.* with any of the different oils. Again, the changes were most
226 pronounced in mice injected with peanut and mineral oil (**Figures 2B and 2F**).

227 Immunohistochemical analysis of CD31-positive endothelial cells revealed an increase
228 in vessel density in the omenta after oil injection. It was strongly increased in the case of peanut
229 and mineral oil but mild in olive and corn oil-treated mice (**Figure 2C and 2G**). In addition,
230 higher numbers of CD11b⁺ myeloid cells were present in all four oil-treated mice, but again,
231 peanut and mineral oil-treated mice had highest infiltration rates (**Figure 2D**).

232 So far, the described changes are indicative of peritoneal inflammation upon local oil
233 injection. Prolonged inflammation may impede tissue healing resulting in organ fibrosis.
234 Indeed, Sirius Red staining revealed an increase in collagen deposition, a typical sign of
235 fibrosis, in the greater omentum of *i.p.* oil-injected mice. Such fibrotic changes were in
236 particular observed in mice treated with peanut and mineral oil (**Figures 2E**).

237 Histopathological scoring of the inflammation grade in the greater omentum by H&E
238 staining was based on the granularity of the tissue, the presence of foamy macrophages or

239 other inflammatory cells, multinucleated giant cells, fibrosis or necrosis with a score from 0 (no
240 inflammation) to 3 (severe chronic inflammation). This showed that *i.p.* injection of all four oils
241 causes xanthogranulomatous inflammation of the omentum with highest scores for mineral
242 and peanut oil. (**Figure 2H**).

243 Similar data were obtained during the analysis of mesentery. The almost transparent
244 membrane became opaque in mice treated *i.p.* with oil. The strongest changes were observed
245 in mice treated with peanut and mineral oil (**Figure 3A**). Lipid droplets in adipocytes of
246 mesentery from mineral oil-treated mice were much smaller compared to controls. Such
247 changes were also observed but to a lesser extent in mice injected *i.p.* with peanut oil, whereas
248 the effects of olive and corn oil were mild (**Figures 3B and 3F**). The number of blood vessels
249 were increased in peanut and mineral oil-treated mice. We detected increased numbers of
250 CD11b⁺ myeloid cells in the mesentery of olive, corn, peanut and to the maximum extent in
251 mineral oil-treated mice (**Figure 3D**). There was mild fibrosis in the mesentery of mice treated
252 with peanut oil and severe fibrosis in mice that had received mineral oil (**Figure 3E**).
253 Histopathological scoring of the inflammation grade revealed that peanut and mineral oil, but
254 not olive and corn oil, generated xanthogranulomatous inflammation (**Figure 3H**).

255 In summary, the histopathological analysis revealed that mineral oil and peanut oil
256 induce a strong xanthogranulomatous inflammatory response in the peritoneum. Olive and
257 corn oils also induce inflammation, but to a much lesser degree.

258

259 **Intraperitoneal oil injection causes myeloid cell infiltration into the peritoneum**

260 To further analyze the immune response, peritoneal lavage was obtained three weeks
261 after the *i.p.* injection. Flow cytometry revealed that the total cell number in the peritoneal
262 lavage was significantly increased in mice treated with either peanut or mineral oil compared
263 to untreated animals (**Figure 4A**). The vast majority of the cell population were myeloid cells
264 (CD45⁺CD19⁻CD11b⁺). Peanut and mineral oil increased the total number of myeloid cells,

265 whereas olive and corn oil had no significant effect (**Figure 4B and Supplementary Figure**
266 **2A**).

267 We also observed that oil injection led to a decrease in the number of B
268 (CD45⁺CD19⁺CD3⁻) and T lymphocytes (CD45⁺CD19⁻CD3⁺) (**Supplementary Figure 2B**).
269 This was expected as during peritoneal inflammation lymphocytes migrate from the peritoneal
270 fluid into the greater omentum (21, 22).

271

272 **Peanut and mineral oil increases neutrophil and monocyte recruitment**

273 A more detailed evaluation of the myeloid population revealed that peanut and mineral
274 oil injection strongly increased the presence of neutrophils (CD45⁺CD11b⁺Ly6G⁺Ly6C^{int}) and
275 recruited monocytes (CD45⁺CD11b⁺Ly6G⁻Ly6C⁺) in the peritoneal fluid. Neutrophils and
276 infiltrated monocytes were almost absent in peritoneal lavage derived from untreated mice or
277 mice treated with olive oil, corn oil or oral gavage (**Figures 4C, D and E**).

278 Importantly, the injection itself did not cause such alterations. Injection of 0.9% NaCl
279 did not lead to macroscopic or histological changes, nor to significant changes in total number
280 of cells in peritoneal fluid or changes within the myeloid cell compartment (**Supplementary**
281 **Figure 3A-G**).

282

283 **Oil injection leads to a severe reduction of resident peritoneal macrophages**

284 During inflammation, neutrophils are the first cells being recruited to clear apoptotic
285 cells or eliminate pathogens. Afterwards, monocytes reach the inflamed zone to eliminate
286 dying neutrophils and to differentiate into macrophages. The latter is in particular essential
287 when resident macrophages are eradicated. Therefore, we next examined the macrophage
288 population within the peritoneum. The total macrophage (CD45⁺CD11b⁺F4/80⁺) cell number
289 was not significantly changed in peritoneal lavage of mice treated *i.p.* with oil compared to the
290 untreated mice or to those which received oil by oral gavage (**Figure 4F**).

291 We further characterized the F4/80 population by analyzing the amount of Tim4 on the
292 cell surface as Tim4 can be employed as a marker to differentiate long-term (F4/80⁺Tim4⁺)
293 from newly recruited (F4/80⁺Tim4⁻) resident macrophages (23). This revealed that all four oils
294 led to a dramatic decrease in long-term resident (F4/80⁺Tim4⁺) macrophages and a
295 replacement by recently recruited (F4/80⁺Tim4⁻) macrophages (**Figure 4G**).

296 The level of F4/80 on the macrophage cell membrane varies depending on the
297 differentiation stage (15). In this regard, resident macrophages express high levels of F4/80,
298 while newly recruited monocyte-derived macrophages express low to intermediate levels
299 (F4/80^{int}). Peanut oil injection led to a strong decrease in resident F4/80^{hi} macrophage numbers
300 (**Figure 4H**). Mineral oil showed a similar but not significant trend, whereas olive oil and corn
301 oil did not alter the proportion of F4/80^{hi} macrophages.

302 The full resolution of inflammation is carried out by F4/80^{int} macrophages (16). Analysis
303 of this cell population revealed that only the *i.p.* injection of olive oil led to a significant increase
304 in F4/80^{int} macrophages at this time point (**Figure 4I**).

305 Collectively, the data imply that injection of any oil into the peritoneum triggers an
306 inflammatory response in which resident macrophages get replaced by monocyte-derived
307 ones. However, the resolution of inflammation depends on the type of oil, with olive oil and
308 corn oil (to a lesser extent) showing signs of resolution.

309

310 **Oil injection induces foam cell formation**

311 Monocytes and macrophages can take up excessive amounts of lipids (24). Therefore,
312 we examined lipid uptake in macrophages upon oil injection. Peritoneal lavage was performed
313 three weeks after *i.p.* oil injection. Adherent peritoneal macrophages were stained with Oil Red
314 O, which marks lipids and neutral triglycerides. Macrophages derived from the control mice
315 were not stained by Oil Red O while peritoneal macrophages derived from mice injected *i.p.*
316 with peanut oil contained multiple large lipid droplets. Fewer amounts were detected in the

Alsina-Sanchis et al., Oil depletes resident peritoneal macrophages

317 macrophages from the olive oil and corn oil group, whereas the macrophages of the mineral
318 oil group contained almost no detectable lipid droplets (**Figure 5A**).

319 To further evaluate this, we tested lipid uptake in the J774A.1 macrophage cell line.
320 J774A.1 macrophages took up lipids when in contact with olive, corn and peanut oil, but not
321 mineral oil, suggesting that the effect of this oil is independent of the cellular lipid uptake.

322 In atherosclerotic plaques, monocyte-derived macrophages endocytose lipids such as
323 oxidized LDL and become foam cells. During this transition, an upregulation of the fatty acid
324 translocase (CD36) expression and downregulation of the cholesterol transporter ABCG1 is
325 evident (25). J774A.1 macrophages showed the same changes in gene expression when
326 cultured for four hours in the presence of vegetal oils (**Figure 5C-F**).

327 In summary, these results indicate that peanut, olive and corn, but not mineral oil *i.p.*
328 injection leads to foam cell formation.

329

330 **Peritoneal macrophage cell death after exposure to different oils**

331 Lipoprotein uptake can cause macrophage cell death (26). Therefore, we evaluated
332 whether peritoneal macrophage cell death is induced by the four different oils. Mice were
333 injected once *i.p.* with 100 μ l oil and five minutes later peritoneal cells were harvested and
334 subjected to flow cytometry (**Figure 6A**). This revealed that compared to untreated mice there
335 was approximately a 50% decrease in CD11b⁺F4/80⁺ macrophages in the peritoneum of mice
336 that received any of the oils (**Figure 6B**). There was a 5-10% decrease in the fraction of live
337 cells (Annexin V⁻, PI⁻) and an equivalent increase of necrotic (PI⁺), apoptotic (Annexin V⁺) and
338 Annexin V⁺PI⁺ cells in the peritoneal lavage of mice that received peanut or olive oil (**Figure**
339 **6C**). The Annexin V⁺PI⁺ double-positive population can be the result of both, apoptosis and
340 necrosis (27). The increase in cell death was milder in the presence of corn oil, whereas in
341 mineral oil injected mice cell death was not different as compared to untreated mice,
342 suggesting that the mechanism for mineral oil-induced injury is different (**Figure 6C**).

343 To further analyze cell death in macrophages, J774A.1 cells were treated with different
344 oils. All three vegetal oils increased cell death. In this case, the increase in Annexin V⁺, PI⁺
345 double positive cells was present for olive, corn and peanut oil. Moreover, necrotic cell death
346 (Annexin V⁻, PI⁺) was also increased in the presence of peanut and corn oil (**Figure 6D**).

347 In order to further clarify whether macrophages die by apoptosis or necrosis we
348 incubated J774A.1 cells with different oils to determine apoptotic and necrotic cell death. There
349 was an increase in apoptotic cells in the case of incubation with olive oil and a mild increase
350 in the presence of corn oil. 7-AAD incorporation (necrosis) was increased upon treatment with
351 peanut and to a lesser extent upon treatment with corn and mineral oil (**Figure 6E-G**).

352 Another way to detect necrotic cell death is measuring lactate dehydrogenase (LDH)
353 activity in the cell culture supernatant. Membrane disruption of necrotic cells allows release of
354 cytosolic LDH. Peanut oil caused pronounced release of LDH. There was also LDH release
355 from macrophages treated with olive and corn oil, however to a lesser degree (**Figure 6H**).
356 Interestingly, the LDH release upon treatment with peanut oil could be strongly decreased by
357 supplementing peanut oil with the polyunsaturated oleic acid (**Supplemental Figure 4A**).

358 We corroborated the different mechanisms of cell death further and observed that only
359 treatment with olive oil induces cleavage of caspase-3 in macrophages, a major effector of
360 apoptosis (**Figure 6J**). On the other hand, peanut oil-treated macrophages showed an
361 increase in active p20 caspase-1, which is a marker for pyroptosis (**Figure 6J-K**), which has
362 similar features as necrosis but is driven by caspase-1 activation (28). In contrast, olive oil-
363 treated macrophages showed increased levels of IL10 and Arginase-1 indicating an anti-
364 inflammatory switch towards resolution of inflammation (**Figure 6I-K**).

365 These results suggest that macrophages in contact with olive oil die by apoptosis,
366 which facilitates the subsequent resolution of the inflammation, whereas peanut oil induces
367 macrophage pyroptosis, which impairs the resolution of inflammation.

368

369 ***I.p.* injection of peanut oil impairs the resolution of inflammation in a peritonitis model**

370 The results presented indicate that *i.p.* oil injection leads to a dramatic change in the
371 peritoneal immune cell composition. Chronic inflammation is induced by peanut oil and this
372 would potentially alter the outcome of experiments executed subsequently. One such example
373 could be a peritonitis experiment in transgenic mice that had been injected *i.p.* before with
374 tamoxifen in peanut oil to induce gene recombination. We decided to test this in experimental
375 peritonitis model, in which mice received peanut oil by *i.p.* injection or by oral gavage as control.
376 Three weeks later, thioglycolate was applied to mimic bacterial peritonitis (**Figure 7A**).

377 It is known that thioglycolate initially induces a massive neutrophil and monocyte
378 infiltration, followed by differentiation into macrophages that resolve inflammation by clearance
379 of apoptotic cells (16). Consistently, mice that had received peanut oil by oral gavage had
380 approximately 50% increase in myeloid cell numbers 24 and 72 hours after thioglycolate
381 injection. However, mice pretreated *i.p.* with oil, already had high numbers of CD45⁺CD11b⁺
382 myeloid cells in peritoneal fluid at baseline and this was not further increased upon
383 thioglycolate administration (**Figure 7C**). In mice treated by oral gavage, the number of
384 monocytes and neutrophils in peritoneal fluid increased strongly upon thioglycolate injection
385 and subsequently returned below baseline. This suggests that the first inflammatory response
386 by these cells had already been cleared. However, in mice that had been *i.p.* injected with
387 peanut oil there was a higher proportion of monocytes and neutrophils already under basal
388 conditions, which was maintained after thioglycolate administration (**Figure 7B and D-E**).

389 Mice treated orally showed the expected increase in CD45⁺CD11b⁺F4/80⁺
390 macrophages 72 hours after thioglycolate injection. However, mice that had been injected *i.p.*
391 with peanut oil had only few macrophages present in the peritoneum (approximately 12% of
392 all myeloid cells) and these increased only marginally (**Figure 7F**). Orally treated mice showed
393 disappearance of F4/80^{hi} macrophages 24 hours after thioglycolate administration and
394 subsequent recovery, which was accompanied by an increase of F4/80^{int} macrophages
395 (**Figure 7G-H**). This suggests that resident macrophages disappear after thioglycolate
396 administration and get replaced by monocyte-derived macrophages as the inflammation
397 resolves. Yet, in mice that received peanut oil *i.p.* there were only few F4/80^{hi} macrophages at

398 baseline and there was only a minor increase in F4/80^{int} macrophages (**Figure 7G-H**). The
399 lower presence of F4/80^{int} macrophages, together with the continuous influx of monocytes and
400 neutrophils, suggests that resolution of inflammation cannot take place. As such, *i.p.* peanut
401 oil injection leads to a dramatic change in the myeloid cell composition of the peritoneum that
402 affects the outcome of subsequent experiments.

403

404 **Discussion**

405 Animal experimentation requires careful planning and analysis to allow reproducibility
406 and the possibility to translate basic research into successful clinical trials. Oil injection is
407 frequently performed in animal research, in particular to deliver tamoxifen for inducible gene
408 recombination (1, 2, 4). Oil is considered to be safe and non-toxic. However, few studies
409 reported peritoneal inflammation after subcutaneous or intraperitoneal oil injection (6, 10, 29).
410 To our knowledge, little is still known about changes in the immune cell composition and related
411 reactions within the peritoneum upon intraperitoneal oil delivery. This work demonstrates that
412 intraperitoneal injection of four different oils causes inflammation, foam cell formation and
413 depletion of resident macrophages. However, the severity of inflammation strongly depends
414 on the type of oil.

415 Within the peritoneum, the omentum plays a major role in recognition and
416 encapsulation of pathogens (30). During this process, it expands, a feature which we observed
417 after injection of the different oils. Interestingly, the applied oils were not completely resorbed
418 even three weeks after injection into the peritoneal cavity. In particular larger amounts of
419 peanut oil were still visible in the peritoneal fluid. The failed clearance can be assumed to
420 prolong the phase of acute inflammation (17). Consistently, chronic xanthogranulomatous
421 inflammation and fibrosis were observed, particularly upon peanut and mineral oil treatment.
422 Myeloid cell infiltration and fibrosis were more severe in the omentum compared to the
423 mesentery. This is consistent with the fact that the omentum is an immunological niche and

424 the first organ to react against pathogens, but only when this inflammation becomes chronic it
425 starts to affect the mesentery (20).

426 Mechanistically, the type of oil-induced macrophage cell death appears to determine
427 whether inflammation gets resolved. For successful resolution of the inflammation, there is the
428 need of efferocytosis, where macrophages engulf apoptotic cells (31). Non-resolving
429 inflammation contributes substantially to the progression of atherosclerotic plaques and other
430 chronic inflammatory diseases (18, 32, 33). Our data indicate that macrophages in contact with
431 olive oil die by apoptosis, which facilitates efferocytosis-mediated resolution of inflammation.
432 Conversely, peanut oil induces pyroptosis of macrophages. Excessive pyroptosis impairs the
433 resolution of inflammation (34, 35). As such, peanut oil injection results in chronic peritoneal
434 inflammation, whereas olive oil induces macrophage apoptosis, followed by efferocytosis and
435 initiation of the resolution phase.

436 At the cellular level, all three vegetal oils were taken up by macrophages and caused
437 foam cell formation. This change in the expression pattern has been observed in peritoneal
438 macrophages isolated from obese mice, and blood monocytes from patients suffering from
439 severe atherosclerosis (36-38). In principle, one could even use intraperitoneal peanut oil
440 injection as a fast model to obtain viable foam cells for *in vitro* experiments. Future research
441 will determine the potential of this model.

442 In conclusion, our study shows that intraperitoneal injection of different oils causes
443 peritoneal inflammation and depletion of resident peritoneal macrophages. Whereas olive oil
444 triggers macrophage apoptosis and resolution of inflammation, peanut oil induces pyroptosis
445 and chronic non-resolved inflammation. This has important consequences for animal
446 experiments. In a proof-of-principle approach, we demonstrated this in a thioglycolate-induced
447 peritonitis model after peanut oil injection. To overcome such limitations, it is advisable to
448 deliver lipophilic substances like tamoxifen by oral gavage instead of intraperitoneal injection.

449

450

451 **Acknowledgements**

452 This work was funded by the Deutsche Forschungsgemeinschaft (DFG) project number
453 394046768 - SFB1366 projects C4 and Z2 (to A.F., C.M.), DFG project number 419966437 (to
454 J.R.V.) and the Helmholtz Association (to A.F.).

455

456 **Conflict of interest**

457 The authors declare that they have no conflict of interest.

458 **References**

- 459 1. Sauer B. Inducible gene targeting in mice using the Cre/lox system. *Methods*. 1998;14(4):381-92.
- 460 2. Feil S, Valtcheva N, Feil R. Inducible Cre mice. *Methods Mol Biol*. 2009;530:343-63.
- 461 3. Scholten D, Trebicka J, Liedtke C, Weiskirchen R. The carbon tetrachloride model in mice. *Lab*
462 *Anim*. 2015;49(1 Suppl):4-11.
- 463 4. Yanguas SC, Cogliati B, Willebrords J, Maes M, Colle I, van den Bossche B, et al. Experimental
464 models of liver fibrosis. *Arch Toxicol*. 2016;90(5):1025-48.
- 465 5. Anderson PN, Potter M. Induction of plasma cell tumours in BALB-c mice with 2,6,10,14-
466 tetramethylpentadecane (pristane). *Nature*. 1969;222(5197):994-5.
- 467 6. Kuroda Y, Akaogi J, Nacionales DC, Wasdo SC, Szabo NJ, Reeves WH, et al. Distinctive patterns of
468 autoimmune response induced by different types of mineral oil. *Toxicol Sci*. 2004;78(2):222-8.
- 469 7. Chen H, Liao D, Cain D, McLeod I, Ueda Y, Guan Z, et al. Distinct granuloma responses in C57BL/6J
470 and BALB/cByJ mice in response to pristane. *Int J Exp Pathol*. 2010;91(5):460-71.
- 471 8. Nacionales DC, Kelly KM, Lee PY, Zhuang H, Li Y, Weinstein JS, et al. Type I interferon production
472 by tertiary lymphoid tissue developing in response to 2,6,10,14-tetramethyl-pentadecane
473 (pristane). *Am J Pathol*. 2006;168(4):1227-40.
- 474 9. Brand C, da Costa TP, Bernardes ES, Machado CM, Andrade LR, Chammas R, et al. Differential
475 development of oil granulomas induced by pristane injection in galectin-3 deficient mice. *BMC*
476 *Immunol*. 2015;16:68.

- 477 10. Ramot Y, Ben-Eliahu S, Kagan L, Ezov N, Nyska A. Subcutaneous and intraperitoneal
478 lipogranulomas following subcutaneous injection of olive oil in Sprague-Dawley rats. *Toxicol*
479 *Pathol.* 2009;37(7):882-6.
- 480 11. Prame Kumar K, Nicholls AJ, Wong CHY. Partners in crime: neutrophils and
481 monocytes/macrophages in inflammation and disease. *Cell Tissue Res.* 2018;371(3):551-65.
- 482 12. Schulz C, Gomez Perdiguero E, Chorro L, Szabo-Rogers H, Cagnard N, Kierdorf K, et al. A lineage of
483 myeloid cells independent of Myb and hematopoietic stem cells. *Science.* 2012;336(6077):86-90.
- 484 13. Barth MW, Hendrzak JA, Melnicoff MJ, Morahan PS. Review of the macrophage disappearance
485 reaction. *J Leukoc Biol.* 1995;57(3):361-7.
- 486 14. Sieweke MH, Allen JE. Beyond stem cells: self-renewal of differentiated macrophages. *Science.*
487 2013;342(6161):1242974.
- 488 15. Cassado Ados A, D'Imperio Lima MR, Bortoluci KR. Revisiting mouse peritoneal macrophages:
489 heterogeneity, development, and function. *Front Immunol.* 2015;6:225.
- 490 16. Gautier EL, Ivanov S, Lesnik P, Randolph GJ. Local apoptosis mediates clearance of macrophages
491 from resolving inflammation in mice. *Blood.* 2013;122(15):2714-22.
- 492 17. Lawrence T, Gilroy DW. Chronic inflammation: a failure of resolution? *Int J Exp Pathol.*
493 2007;88(2):85-94.
- 494 18. Kasikara C, Doran AC, Cai B, Tabas I. The role of non-resolving inflammation in atherosclerosis. *J*
495 *Clin Invest.* 2018;128(7):2713-23.
- 496 19. Xu S, Huang Y, Xie Y, Lan T, Le K, Chen J, et al. Evaluation of foam cell formation in cultured
497 macrophages: an improved method with Oil Red O staining and DiI-oxLDL uptake. *Cytotechnology.*
498 2010;62(5):473-81.
- 499 20. Meza-Perez S, Randall TD. Immunological Functions of the Omentum. *Trends Immunol.*
500 2017;38(7):526-36.
- 501 21. Carlow DA, Gold MR, Ziltener HJ. Lymphocytes in the peritoneum home to the omentum and are
502 activated by resident dendritic cells. *J Immunol.* 2009;183(2):1155-65.

- 503 22. Laurin LP, Brissette MJ, Lepage S, Cailhier JF. Regulation of experimental peritonitis: a complex
504 orchestration. *Nephron Exp Nephrol.* 2012;120(1):e41-6.
- 505 23. Bain CC, Hawley CA, Garner H, Scott CL, Schridde A, Steers NJ, et al. Long-lived self-renewing bone
506 marrow-derived macrophages displace embryo-derived cells to inhabit adult serous cavities. *Nat*
507 *Commun.* 2016;7:ncomms11852.
- 508 24. Remmerie A, Scott CL. Macrophages and lipid metabolism. *Cell Immunol.* 2018;330:27-42.
- 509 25. Rahaman SO, Lennon DJ, Febbraio M, Podrez EA, Hazen SL, Silverstein RL. A CD36-dependent
510 signaling cascade is necessary for macrophage foam cell formation. *Cell Metab.* 2006;4(3):211-21.
- 511 26. Seimon TA, Nadolski MJ, Liao X, Magallon J, Nguyen M, Feric NT, et al. Atherogenic lipids and
512 lipoproteins trigger CD36-TLR2-dependent apoptosis in macrophages undergoing endoplasmic
513 reticulum stress. *Cell Metab.* 2010;12(5):467-82.
- 514 27. Ormerod MG. The study of apoptotic cells by flow cytometry. *Leukemia.* 1998;12(7):1013-25.
- 515 28. Yuan J, Najafov A, Py BF. Roles of Caspases in Necrotic Cell Death. *Cell.* 2016;167(7):1693-704.
- 516 29. Hubbard JS, Chen PH, Boyd KL. Effects of Repeated Intraperitoneal Injection of Pharmaceutical-
517 grade and Nonpharmaceutical-grade Corn Oil in Female C57BL/6J Mice. *J Am Assoc Lab Anim Sci.*
518 2017;56(6):779-85.
- 519 30. Litbarg NO, Gudehithlu KP, Sethupathi P, Arruda JA, Dunea G, Singh AK. Activated omentum
520 becomes rich in factors that promote healing and tissue regeneration. *Cell Tissue Res.*
521 2007;328(3):487-97.
- 522 31. Boada-Romero E, Martinez J, Heckmann BL, Green DR. The clearance of dead cells by
523 efferocytosis. *Nat Rev Mol Cell Biol.* 2020.
- 524 32. Schrijvers DM, De Meyer GR, Kockx MM, Herman AG, Martinet W. Phagocytosis of apoptotic cells
525 by macrophages is impaired in atherosclerosis. *Arterioscler Thromb Vasc Biol.* 2005;25(6):1256-
526 61.
- 527 33. Schett G, Neurath MF. Resolution of chronic inflammatory disease: universal and tissue-specific
528 concepts. *Nat Commun.* 2018;9(1):3261.

- 529 34. Bergsbaken T, Fink SL, Cookson BT. Pyroptosis: host cell death and inflammation. *Nat Rev*
530 *Microbiol.* 2009;7(2):99-109.
- 531 35. Wu J, Lin S, Wan B, Velani B, Zhu Y. Pyroptosis in Liver Disease: New Insights into Disease
532 Mechanisms. *Aging Dis.* 2019;10(5):1094-108.
- 533 36. Mauldin JP, Srinivasan S, Mulya A, Gebre A, Parks JS, Daugherty A, et al. Reduction in ABCG1 in
534 Type 2 diabetic mice increases macrophage foam cell formation. *J Biol Chem.*
535 2006;281(30):21216-24.
- 536 37. Piechota M, Banaszewska A, Dudziak J, Slomczynski M, Plewa R. Highly upregulated expression of
537 CD36 and MSR1 in circulating monocytes of patients with acute coronary syndromes. *Protein J.*
538 2012;31(6):511-8.
- 539 38. Chistiakov DA, Melnichenko AA, Myasoedova VA, Grechko AV, Orekhov AN. Mechanisms of foam
540 cell formation in atherosclerosis. *J Mol Med (Berl).* 2017;95(11):1153-65.

1 **Figure legends**

2 **Figure 1. Macroscopic changes in mice three weeks after *i.p.* oil injection. A.** Schematic
3 illustration of the *i.p.* or oral oil administration protocol. **B.** Representative images of the
4 peritoneum. Black arrows indicate visible lipid droplets. White arrowheads mark nodules on
5 the surface of organs. Scale bar, 3 mm. **C.** Representative microscopic images of liver sections
6 stained with H&E. Xanthogranuloma on the liver surface in mice treated with peanut and
7 mineral oil. Scale bar, 50 μ m.

8

9 **Figure 2. Xanthogranulomatous inflammation in the omentum upon oil injection.**

10 **A.** Representative images of omenta from untreated mice and such that were treated with oil
11 by *i.p.* injection or oral gavage. Analysis was performed three weeks after treatment. **B.**
12 Representative confocal images of mesentery sections stained with H&E. Scale bar, 50 μ m.
13 **C.** Immunofluorescence microscopy to detect CD31⁺ endothelial cells (white). Scale bar 20
14 μ m. **D.** CD11b⁺ myeloid cells. Scale bar, 100 μ m. **E** Sirius Red staining to detect fibrosis. Scale
15 bar, 100 μ m. **F.** Lipid droplet size quantification from H&E images. Untreated mice n=3, peanut
16 oil n=4, olive oil n=3, corn oil n=5, mineral oil n=5 and oral gavage n=3. Bar graphs show
17 mean \pm SD, *, p<0.05 (one way ANOVA). **G.** Quantification of microvessel density. Olive oil
18 n=4 and all other groups n=5. Bar graphs show mean \pm SD, *, p<0.05 (one way ANOVA). **H.**
19 Xanthogranulomatous inflammation score. 0: no inflammation to 3: very strong inflammation.
20 All data represent n=5 mice, bar graphs show mean \pm SD, *, p<0.05 (one way ANOVA).

21

22 **Figure 3. Xanthogranulomatous inflammation in the mesentery upon peanut and**

23 **mineral oil injection. A.** Representative images of mesentery from untreated mice and such
24 that were treated with oil by *i.p.* injection or oral gavage. Analysis was performed three weeks
25 after treatment. **B.** Representative confocal images of mesentery sections stained with H&E.
26 Scale bar, 50 μ m. **C.** Immunofluorescence microscopy to detect CD31⁺ endothelial cells
27 (white). Scale bar, 20 μ m **D.** CD11b⁺ myeloid cells. Scale bar, 100 μ m **E** Sirius Red staining to

Alsina-Sanchis et al., Oil depletes resident peritoneal macrophages

28 detect fibrosis. Scale bar, 100 μ m **F.** Lipid droplet size quantification from H&E images. n=3
29 mice. Bar graph shows mean \pm SD, *, p<0.05 (one way ANOVA). **G.** Quantification of
30 microvessel density. n=5 mice. Bar graph shows mean \pm SD, *, p<0.05 (one way ANOVA). **H.**
31 Xanthogranulomatous inflammation score. 0: no inflammation to 3: very strong inflammation.
32 Olive oil n=4 and all other groups n=5. Bar graph shows mean \pm SD, *, p<0.05 (one way
33 ANOVA).

34

35 **Figure 4. Resident peritoneal macrophage depletion and persistent monocyte and**
36 **neutrophil infiltration upon peanut and mineral oil injection.** Peritoneal lavage (PL) was
37 obtained three weeks after treatment with oil. **A.** Total cell number in peritoneal lavage **B.**
38 Myeloid cells (CD45⁺CD11b⁺) in peritoneal lavage. **C.** Neutrophils
39 (CD45⁺CD11b⁺Ly6G⁺Ly6C^{int}) in peritoneal lavage. **D.** Monocytes (CD45⁺CD11b⁺Ly6G⁻Ly6C⁺)
40 in peritoneal lavage. **F.** Macrophages (CD45⁺CD11b⁺F4/80⁺) in peritoneal lavage. **E.**
41 Representative blots of flow cytometry analysis of monocytes, neutrophils and macrophages.
42 **G.** Percentage of CD45⁺CD11b⁺F4/80⁺Tim4⁺ and CD45⁺CD11b⁺F4/80⁺Tim4⁻ macrophages. **H.**
43 Percentage of CD45⁺CD11b⁺F4/80^{hi} macrophages. **I.** Percentage of CD45⁺CD11b⁺F4/80^{int}
44 macrophages. All data represent n=4 mice for untreated, peanut, corn and mineral groups and
45 n=5 for olive and oral gavage groups. Bar graphs show mean \pm SD, *, p<0.05 (one way
46 ANOVA).

47

48 **Figure 5. Macrophage foam cell formation upon contact with vegetal oil.** **A.** Isolation of
49 peritoneal macrophages from untreated mice and three weeks after peanut, olive, corn,
50 mineral oil intraperitoneal injection. Cells from peritoneal lavage were plated for 30 minutes
51 and stained with Oil Red O. Scale bar, 5 μ m. **B.** J774A.1 macrophages after four hours in
52 contact with the different oils. Representative images of Oil Red O staining. Scale bar, 50 μ m.
53 **C.** Representative Western blot of CD36 expression in J774A.1 macrophages after four hours
54 in contact with the different oils. **D.** Representative Western blot of ABCG1 expression in

Alsina-Sanchis et al., Oil depletes resident peritoneal macrophages

55 J774A.1 macrophages after four hours in contact with the different oils. **E.** Quantification of
56 CD36 and ABCG1 mRNA expression levels expression in J774A.1 macrophages after four
57 hours in contact with the different oils. Fold change in comparison to untreated cells. All data
58 from n=3 biological replicates, bar graphs represent mean \pm SD, *, p<0.05 (one way ANOVA).

59

60 **Figure 6. Macrophage cell death upon exposure to vegetal oil. A.** Schematic illustration of
61 *i.p.* oil administration. Peritoneal lavage was obtained five minutes later. **B.** Percentage of
62 macrophages (CD45⁺CD11b⁺F4/80⁺). Untreated mice n=3, peanut oil n=6 mice and all other
63 groups n=5 mice, mean \pm SD, *, p<0.05 (one way ANOVA). **C.** Percentage of live (Annexin V⁻
64 PI⁻), apoptotic (Annexin V⁺PI⁻), necrotic (Annexin V⁻PI⁺) or double positive (Annexin V⁺PI⁺) cells
65 from total number of cells in peritoneal lavage. Untreated mice n=6, peanut and olive oil n=9
66 mice, corn and mineral oil n=10 mice, bar graphs represent mean \pm SD, *, p<0.05 (2-way
67 ANOVA). **D.** J774A.1 macrophage cell line untreated or incubated with different oils for four
68 hours and analysis of the percentage of live (Annexin V⁻PI⁻), apoptotic (Annexin V⁺PI⁻), necrotic
69 (Annexin V⁻PI⁺) or double positive (Annexin V⁺PI⁺) cells. n=3 biological replicates, bar graphs
70 represent mean \pm SD, *, p<0.05 (2-way ANOVA). **E.** J774A.1 macrophages untreated or
71 incubated with different oils for two hours. Quantification positive cells per field in comparison
72 to untreated, blue (alive cells), green (apoptotic) and red (necrotic). n=3 biological replicates,
73 mean \pm SD, *, p<0.05 (one-way ANOVA). **H.** LDH activity in the supernatant upon treatment
74 of J774A.1 macrophages for two hours. n=3 biological replicates, mean \pm SD, *, p<0.05 (one-
75 way ANOVA). **I.** Normalized mRNA expression levels of IL10. n=4 biological replicates,
76 mean \pm SD, *, p<0.05 (one-way ANOVA). **J.** Representative Western blot cleaved caspase-3,
77 arginase-1 and active p20 caspase-1 of J774A.1 macrophages untreated or incubated for four
78 hours with different oils. **K.** Quantification of Western blots. n=3 biological replicates,
79 mean \pm SD, *, p<0.05 (one-way ANOVA).

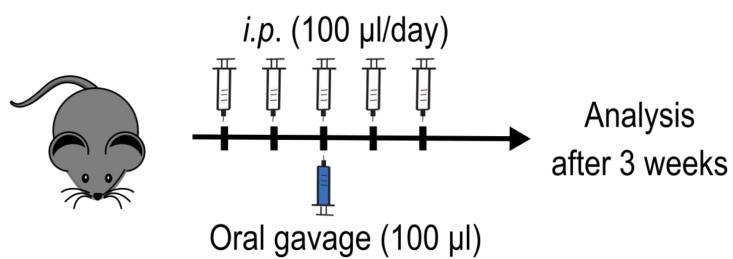
80

Alsina-Sanchis et al., Oil depletes resident peritoneal macrophages

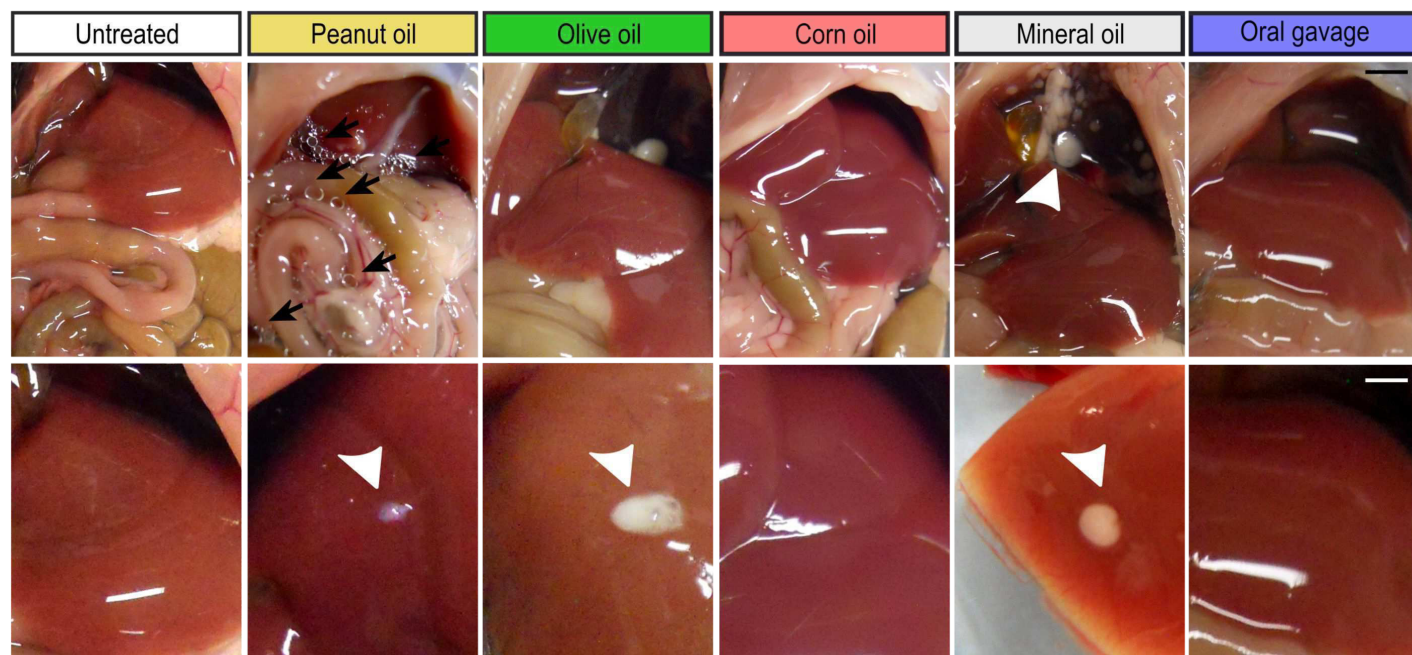
81 **Figure 7. Intraperitoneal injection of peanut oil impairs the resolution of inflammation in**
82 **a thioglycolate-induced peritonitis model. A.** Schematic illustration of *i.p.* or oral oil
83 administration followed by thioglycolate *i.p.* injection three weeks after treatment with oil. **B.**
84 Representative blots of flow cytometry analysis of monocytes, neutrophils. **C.** Percentage of
85 myeloid cells (CD45⁺CD11b⁺) in peritoneal lavage. **D.** Percentage of neutrophils
86 (CD45⁺CD11b⁺Ly6G⁺Ly6C^{int}) in peritoneal lavage. **E.** Percentage of monocytes in peritoneal
87 lavage. **F.** Percentage of macrophages (CD45⁺CD11b⁺F4/80⁺) in peritoneal lavage. **G.**
88 Percentage of macrophages CD45⁺CD11b⁺F4/80^{hi} in peritoneal lavage. **I.** Percentage of
89 macrophages CD45⁺CD11b⁺F4/80ⁱⁿ in peritoneal lavage. n=3 mice for oral gavage followed
90 by thioglycolate and analysis at 24 hours. All other groups n=4 mice.

91

A



B



C

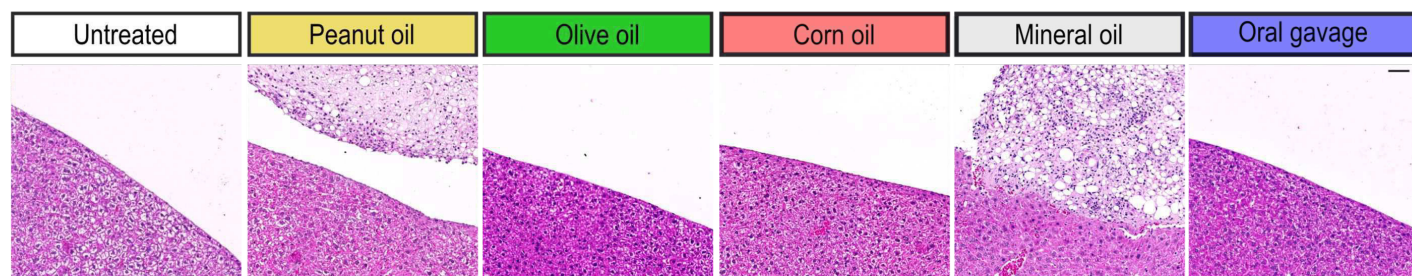


Figure 1

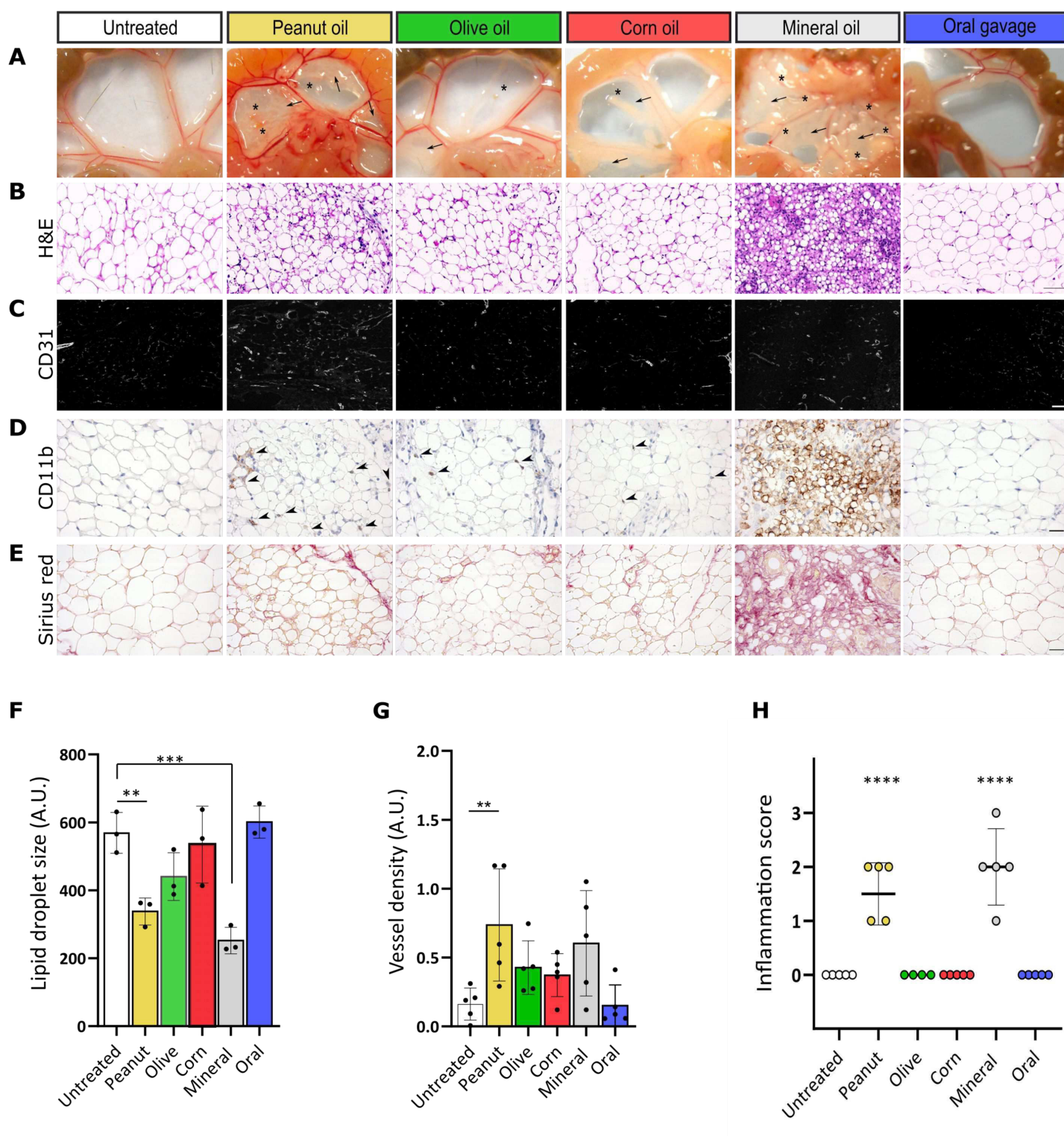


Figure 3

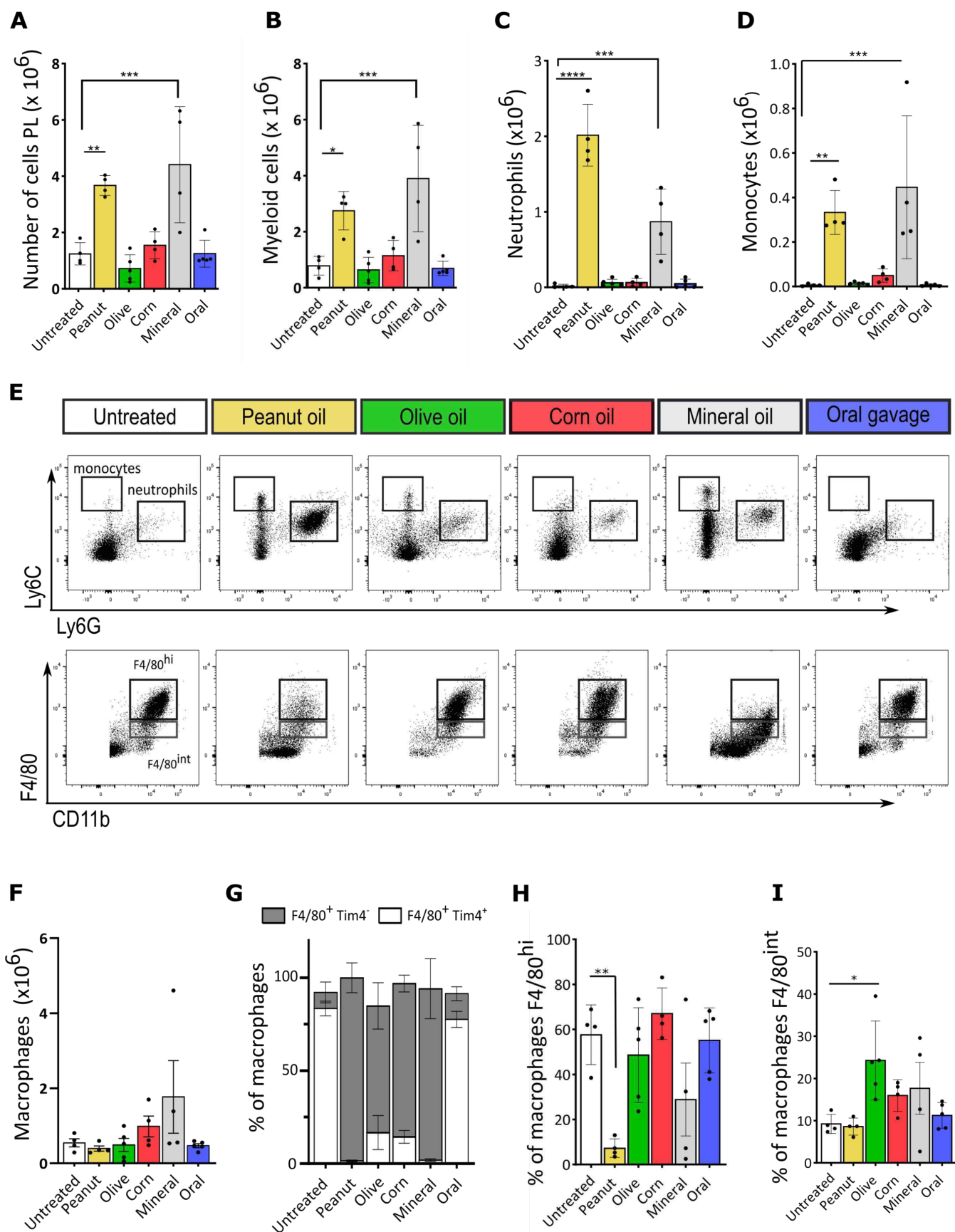
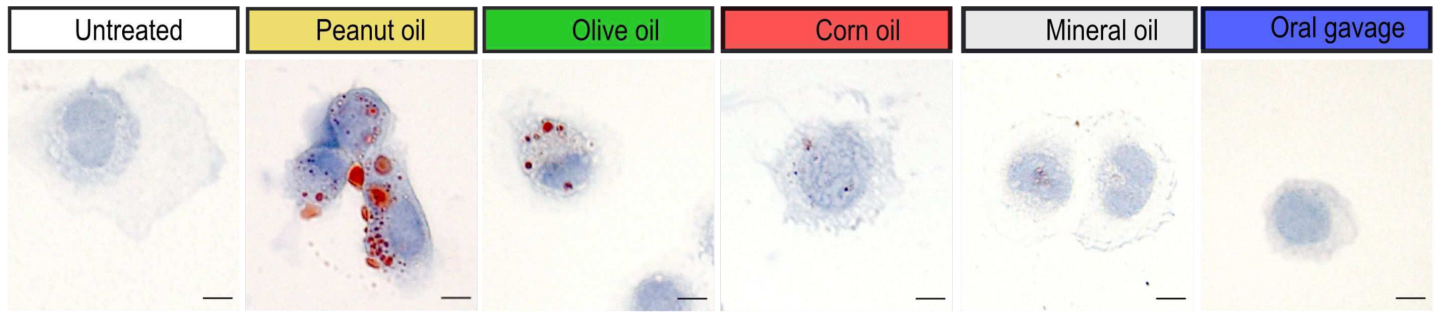
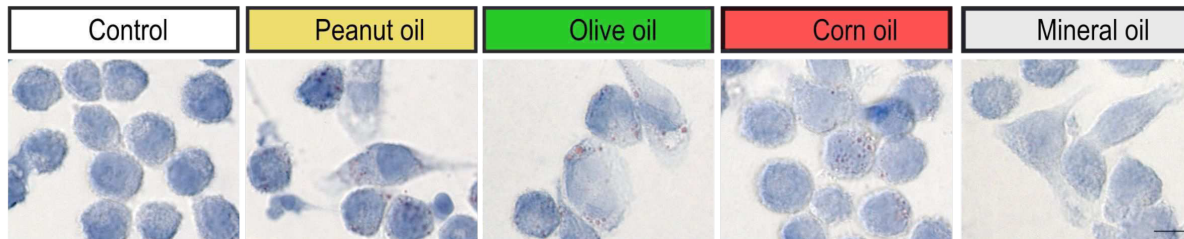


Figure 4.

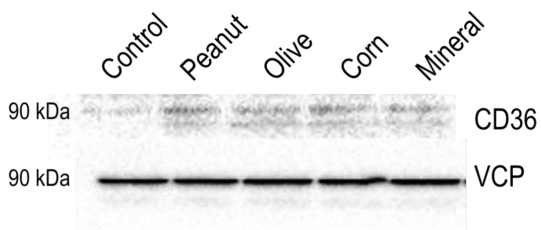
A



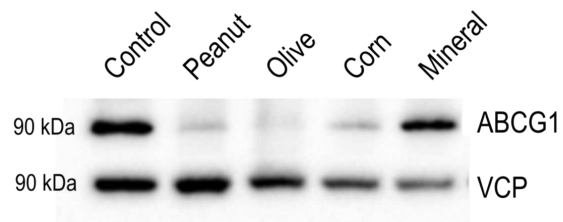
B



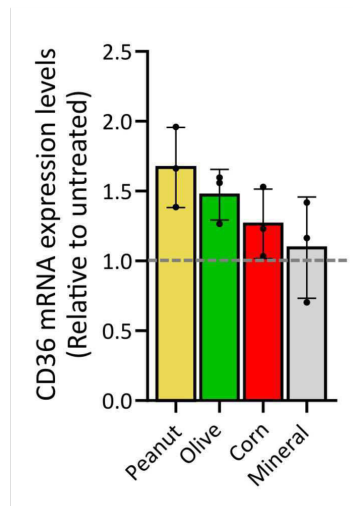
C



D



E



F

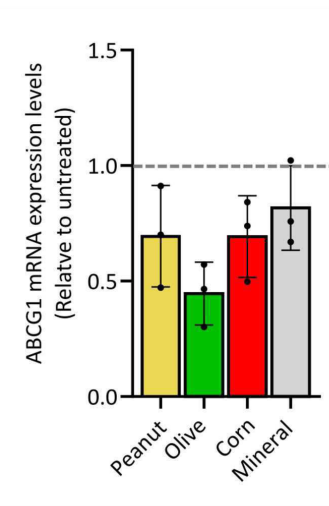


Figure 5.

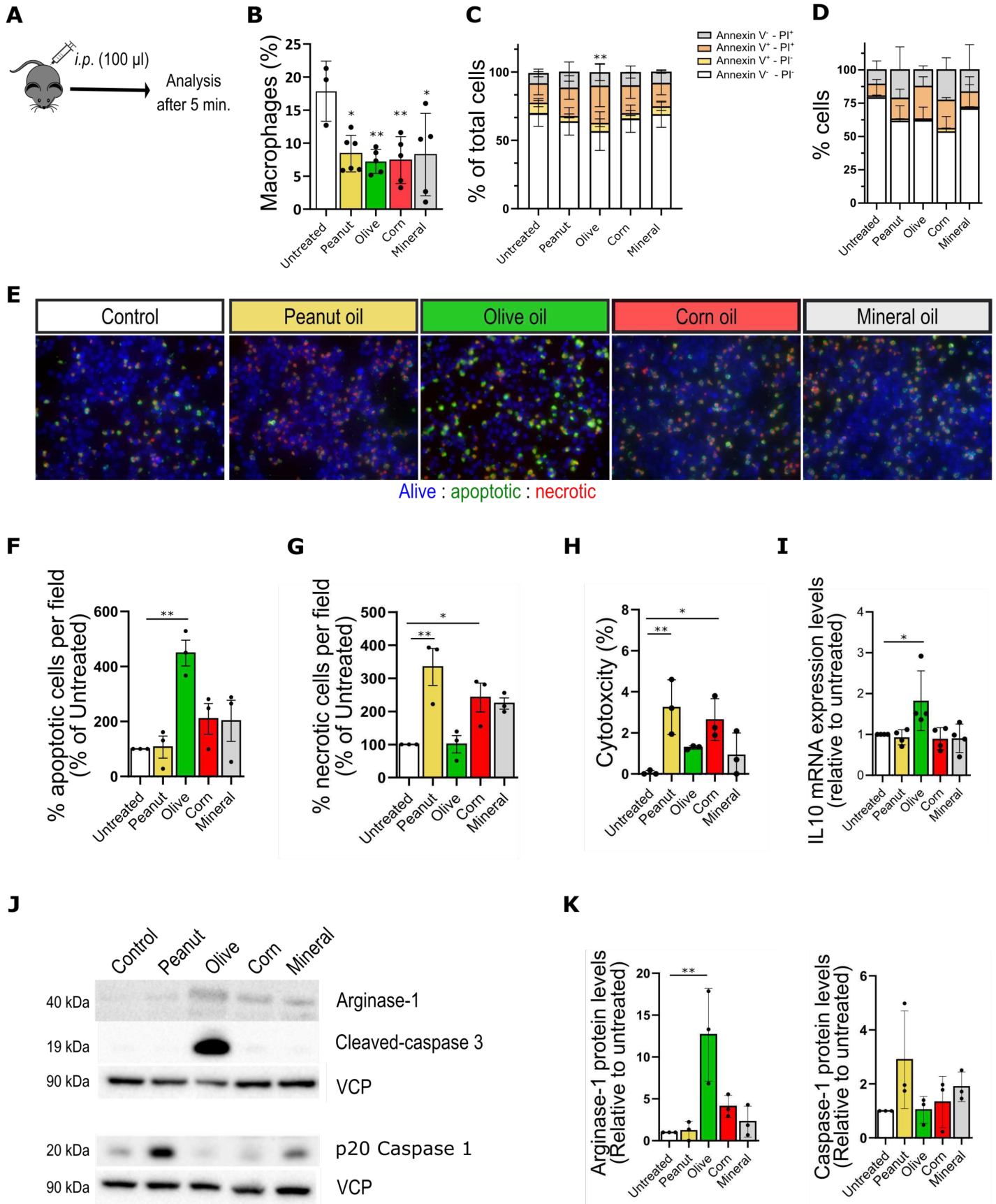


Figure 6.

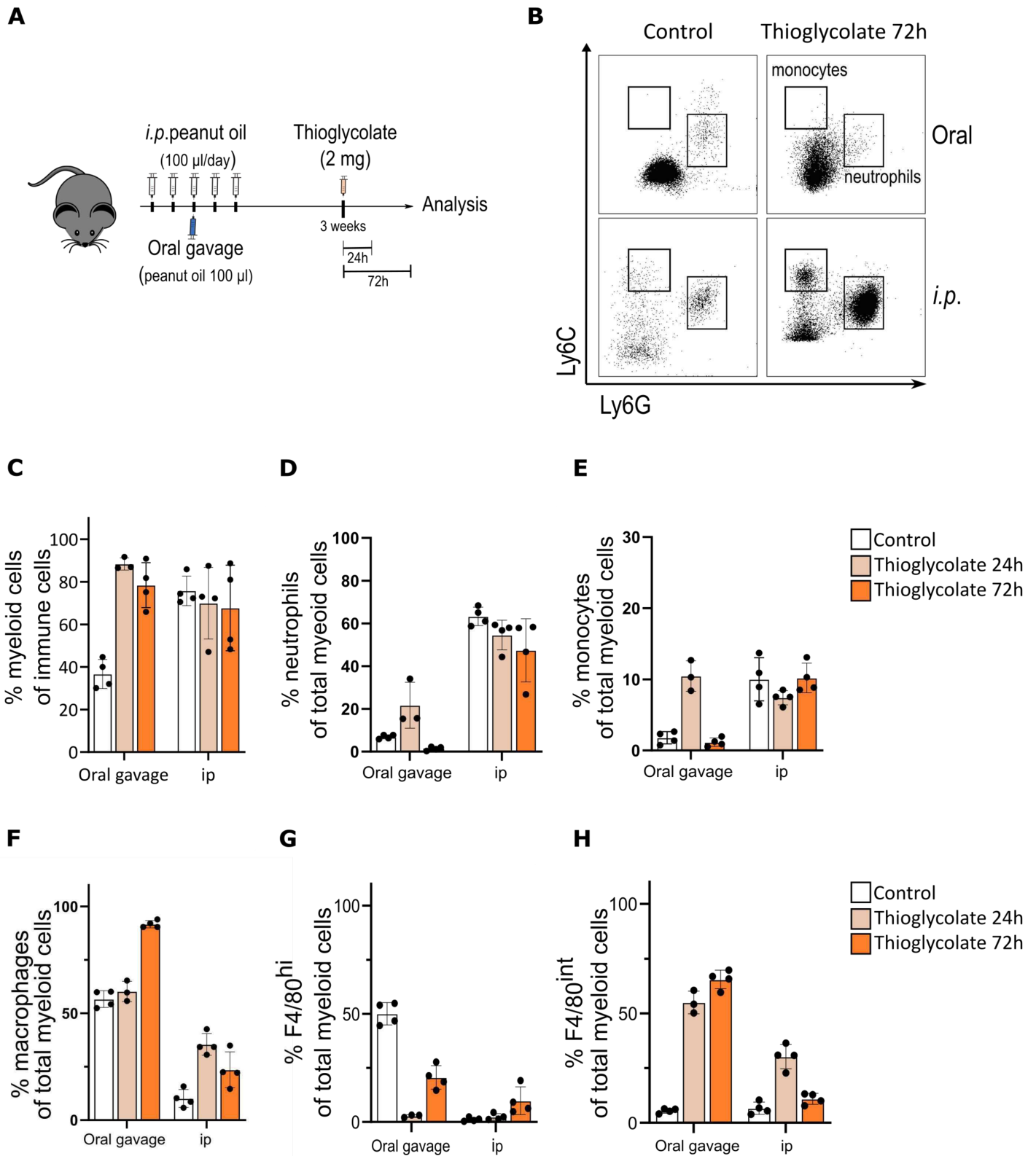


Figure 7.